*J. Nanosci. Nanotechnol. 18, 5854–5857, **2018*** **DOI:** 10.1166/jnn.2018.15385

Does the abiotic formation of oligopeptides on TiO_2 nanoparticles requires special catalytic sites? Apparently not

Marco Fabbiani,[a]* Marco Pazzi,[b] Marco Vincenti,[b] Gloria Tabacchi,[a] Ettore Fois,[a] Gianmario Martra[b]

[a] Department of Science and High Technology and INSTM, University of Insubria, via Valleggio 9, 22100 Como, Italy

[b] Department of Chemistry, University of Torino, via P. Giuria 7, 10125 Torino, Italy

Submitted/Received: 09/10/2017 Accepted: 27/10/2017

* Corresponding author: mfabbiani@uninsubria.it
tel. +39 031 238 6618
ORCID: 0000-0002-9094-0279

The oligomerization of non-activated aminoacids catalyzed by nanostrucrured mineral oxide surfaces holds promises as a sustainable route for the industrial production of polypeptides. To analyze the influence of the surface type on the catalytic process, we performed, via a mild Chemical Vapor Deposition approach, the oligomerization of Glycine on two samples of TiO_2 nanoparticles characterized by different relative amounts of defective surface terminations. Based on infrared spectroscopy and mass spectrometry data, we show herein that the formation of peptide bonds on titania nanoparticles does not require highly energetic surface terminations, but can occu r also on the most abundant and thermodynamically most stable {101} facets of nanosized anatase.

Keywords: TiO_2 nanoparticles, glycine, peptide, prebiotic chemistry, aminoacids CVD.

Abstract

The formation of peptides in mild conditions from non-activated amino acids is an intriguing chemical process potentially providing fundamental insight on the formation of the first biomolecules in abiotic conditions.[1, 2] Additionally, this type of reactions is a relevant proof-of-principle when investigating innovative sustainable routes for the production of peptides and polypeptides of interest in fine chemistry.[3, 4] The thermal condensation of non-activated amino acids was found to be effective under non catalytic anhydrous conditions by using trifunctional amino acids crystals mixtures.[5] When considering a possible influence of the mineral surfaces, Bernal's hypothesis accounts for the potential role of prebiotic surfaces to concentrate and catalyze the amino acids condensation.[6] In this respect, the interaction of both activated and non-activated amino acids with the surface of various solids have been studied[2, 7, 8] and oxide materials received particular attention.[8-12] Independently on the nature of the catalyst, a common difficulty still remains in the production of long oligopeptides when using non-activated amino acids, typically resulting in the production of short oligomers limited to 6 units.[13, 14] However, in 2014 Martra et al. successfully developed an efficient chemical vapor deposition method to obtain at mild conditions (433 K) homopeptides long up to 16 units from non-activated glycine (Gly) when sublimated on amorphous silica and titania.[15] These oxides were used in the form of nanoparticles, thus exposing a specific surface area (SSA) high enough to allow the process to proceed effectively. Nevertheless, nanosizing not only increases the surface/bulk atom ratio, but also the proportion of surface atoms on low energy facets and those on more energetic facets and on edges and corners. Noticeably, surface sites in these three last locations are the most chemically active, because of their peculiar electronic and coordinative state.[16, 17] This would imply a limited number of surface catalytic active sites, which could be beneficial for selectivity, but detrimental for conversion. In the case of the formation of polypeptides in prebiotic conditions, this aspect could represent an additional factor decreasing the probability of the occurrence of the reaction of interest at the surface of minerals. On the other hand, also the technological exploitation of peptide synthesis catalyzed by oxide nanoparticles could benefit by the absence of constraints dealing with the presence of peculiar surface sites. The scientific motivation of this work was actually to address such a question, namely - Are minority sites at oxides surfaces required for the peptide bond formation? A general answer would require the investigation of different types of oxides nanomaterials, covering the whole spectrum of chemical bonding in solids ranging from fully ionic to fully

covalent. As a first contribution to answering the question above, we tested the oligomerization of Gly on two types of TiO_2 nanoparticles (hence a semiconducting material with an ionic-covalent bond character) selected on the basis of their different relative amount of {101} facets, the most thermodynamically stable[18] and more defective surface terminations. Namely, shape-controlled TiO_2 nanoparticles lab-prepared by hydrothermal synthesis (100% anatase, SSA_{BET} ~ 42 m^2 g^{-1}, hereafter TiO_2 HT)[19] and commercial TiO_2 P25 (by Evonik, ~80 % anatase and ~20 % rutile w/w, purity ≥ 99.5 wt%, SSA_{BET} ~ 50 m^2 g^{-1}) were used. Previous investigations demonstrated that the rutile phase account only for ca. 7 % of the SSA of TiO_2 P25.[20] Representative HR-TEM high magnification images of the borders of the two types of nanoparticles are shown in Figure 1. In both cases, {101} lattice fringes are present, running parallel to the main borders which in the case of TiO_2 P25 appear heavily stepped (panel A), whereas for TiO_2 HT are quite flat and regular. These features can be extended to {101} facets: because of the 2D projection character of TEM, and the extremely short wavelength of the electron beam used for imaging (microscope Jeol 3010 operated at 300 kV), borders parallel to lattice fringes due to a crystallographic planes family correspond to the profile of facets terminated by those planes.

Although informative, TEM inspection cannot easily provide insight on all types of surface terminations and their relative abundance, thus the surface features of the two types of TiO_2 nanoparticles are investigated by IR spectroscopy of adsorbed CO (Figure 2), being this molecule a highly sensitive probe to the coordinative state of surface Ti^{4+} ions.[19, 21] Before CO adsorption, titania nanoparticles were outgassed under high dynamic vacuum (residual pressure: $1 \cdot 10^{-5}$ mbar) and re-oxidized at the same temperature by contact with O_2 at 10 mbar in order to obtain an highly de-hydroxylated and fully dehydrated surface.[22]

The spectrum of CO at 45 mbar is dominated by the peak at 2179 cm^{-1} for TiO_2 P25 (panel A) and 2178 cm^{-1} for TiO_2 HT (panel B) typical of these probe molecules adsorbed on {101} TiO_2 anatase surfaces, where Ti^{4+} ions are pentacoordinated.[20] The progressive up-shift of these signals by decreasing the CO coverage is due to the fading away of adsorbate-adsorbate interactions.[21] Moreover, in the case of TiO_2 P25 also a heavy shoulder at 2183 cm^{-1}, due to the presence of CO on {110} TiO_2 anatase surfaces exposing tetracoordinated Ti^{4+} sites,[19] is present, as well as a very weak band at 2206-2208 cm^{-1}, indicating the presence of a few highly coordinatively unsaturated Ti^{4+} sites , generally called “α sites”.[23, 24] The additional weak band at 2212 cm^{-1}, more sensitive to CO outgassing, is due to the combination of the internal stretching mode and a frustrated

translational mode of CO molecules adsorbed on {101} surfaces.[25] Conversely, the spectra of CO adsorbed on TiO_2 HT appear definitely simpler, the main band due to CO on {101} facets being accompanied by a very weak signal due to CO on {110} terminations, while the component produced by CO on α sites is not detectable. Hence, these findings confirm and further underline that there is a significant difference in the surface structure of the two types of titania nanopowders: TiO_2 HT nanoparticles are overwhelmingly terminated by the most stable, highly regular {101} facets exposing pentacoordinated Ti^{4+} sites and two and three fold coordinated oxygen atoms, whereas TiO_2 P25 nanoparticles are also terminated by {110} surfaces, exposing tetracoordinated Ti^{4+} sites and two fold coordinated oxygen atoms,[26] and by a not negligible amount of α sites characterized by Ti^{4+} centers with a stronger Lewis acidity.[23, 24]

In summary, IR spectroscopy of adsorbed CO indicated that TiO_2 HT nanoparticles are overwhelmingly terminated by {101} surfaces, that, as observed by HR-TEM,[25] are the facets of highly regular truncated bipyramidal nanoparticles, ca. 60 nm in length and ca. 30 nm wide. The large prevalence of {101} terminations revealed by IR spectra of adsorbed CO also for TiO_2 P25, and the similar specific surface area with respect to TiO_2 HT, allow to depict also these nanoparticles as truncated bipyramids similar in size to the previous ones, but exposing a significant extent of {110} facets at the intersection of {101} ones at the middle plan of bipyramids.

IR spectroscopy in controlled atmosphere was also used to investigate the fate of Gly molecules adsorbed on titania nanoparticles from the vapor phase, using the protocol set up in a previous work.[15]

Curves a in Figure 3 are the spectra of bare TiO_2 P25 and TiO_2 HT (panel A and B, respectively) outgassed at 433 K in order to dehydrate the nanoparticles. After such treatment, only the typical pattern due to surface OH groups is present in the 3800-3500 cm^{-1} range of the spectrum of TiO_2 P25,[26, 27] whilst for TiO_2 HT this pattern is accompanied by an intense narrow peak at 2345 cm^{-1} and a series of signals in the 1600-1250 cm^{-1} range, due to CO_2 molecules and carboxylates/carbonates species remained entrapped in the inner closed cavities formed in the bulk of nanoparticles during the synthesis.[20] When increasing amounts of Gly are adsorbed from the vapor phase on nanoparticles of both types, a typical pattern of polypeptides appears, with νNH amide bands in the 3500-3000 cm^{-1} and amide I and amide II signals at ca. 1670 cm^{-1} and 1560 cm^{-1}, respectively (curves b-c). In addition, the νCH_2 signals progressively grow in the 3000-2800 cm^{-1} range. The Gly coverage was limited to ca. 60 % of Ti^{4+} surface sites, in order to avoid possible reactions among amino

acid molecules not in interaction with the surfaces of nanoparticles. The coverage was monitored by exploiting a competitive assay with CO_2 dosed at room temperature as probe molecule of Ti^{4+} surface sites[15] (data not shown). Thus, both TiO_2 P25 and TiO_2 HT nanoparticles appeared able to catalyze the condensation among adsorbed amino acids. Noteworthy, a possible catalytic role of rutile nanoparticles in TiO_2 P25 appears not to be relevant, because of the appreciable reactivity already exhibited by pure anatase TiO_2 HT nanoparticles. The relevant but qualitative evidence of the equivalence in reactivity towards amino acids of the TiO_2 nanoparticles differing in surface texture was extended by determining the length of peptides species produced. To this aim, titania samples reacted with Gly are washed with water and the resulting solutions are analyzed by HR-MS. Again, very similar results are obtained for Gly on TiO_2 P25 and TiO_2 HT (Figure 4): in both cases, oligomers long up to 16 units are detected with an overall m/z distribution peaked in correspondence of the Gly 4-mer (m/z = 247). Difference in the relative amount of peptides shorter that 4-mer, as well as of the monomer, are present in the two cases. However, the established method and set up for the sublimation of amino acids and for the contact of their vapours with the nanoparticles does not allow, at present, a control of the reaction conditions fine enough to exclude other factors (different diffusion of amino acids molecules within the pellet of nanoparticles, small fluctuation of the temperature during sublimation) other than surface features played a role in determining the difference in relative amount of shorter oligomers and unreacted monomer.

The collection of data presented allows to conclude that the formation of peptide bonds from non-activated amino acids adsorbed on titania nanoparticles does not require surface sites on highly energetic surface terminations, but occurs on the most stable facets, which are also the most abundant ones. This conclusion usion might not be extended straightforwardly to other oxide catalysts with a significantly different chemical bond character, like silica, because the surface texture resulting from siloxane bridges and silanol groups might change the role of defective towards regular surface sites with respect to what here obtained for titania. Nevertheless, this finding appears to be relevant both for the elucidation of the catalytic role of nanosized minerals towards the formation of peptides in prebiotic era and for the possible technological exploitation of nanosized oxides as heterogeneous catalysts for the production of peptides. Difference in the catalytic activity of anatase TiO_2 nanoparticles toward non-activated amino acid condensation can be expected for

nanoparticles with particular morphologies, resulting from preparation methods favoring the exposure of surface terminations different from the most stable {101} ones.

Acknowledgments

TiO_2 HT nanoparticles are among the outcomes of the FP7 project SetNanoMetro (CA n.604577; www.setnanometro.eu).

Figure 1. HR-TEM images of TiO_2 P25 (panel A) and TiO_2 HT (panel B); original magnifications: x500 k and x800 k respectively. The interfringes distance of 0.352 nm corresponds to the distance between {101} crystal planes in anatase TiO_2 (JCDDS00-021-1272).

Figure 2. FT-IR spectra, in the νCO region, of TiO_2 P25 (panel A) and TiO_2 HT (panel B) outgassed and re-oxidized at 873 K and contacted at 100 K with decreasing CO pressures (from 45 mbar to complete outgassing; lettering in the sense of decreasing coverages). Spectra are reported in Absorbance, after having subtracted the spectra of titania nanoparticles before CO admission as a background.

Figure 3. FT-IR spectra resulting from Gly adsorption from vapor phase on TiO_2 P25 (panel A) and TiO_2 HT (panel B). Curves a: TiO_2 nanoparticles dehydrated by outgassing at 433 K; curves from b to c: after contact with increasing doses of Gly vapors produced by sublimation at 433 K.

Figure 4. ESI-MS spectra of solutions resulting from washing (with pure water) of titania nanoparticles contacted with Gly vapors for 60 min. Panel A: TiO_2 P25; panel B: TiO_2 HT. Numbers on the bars in panel A are the m/z values (without decimal digits for the sake of clarity) of $(\text{-Gly-})_n$ peptides; labels on the bars in panel B are the number of terms in $(\text{-Gly-})_n$ peptides. The difference in m/z values between consecutive signals is 57, corresponding to a Gly peptide unit. Detection conditions resulted in the protonation of analyzed species (m/z values increased of one unit with respect to original analytes).

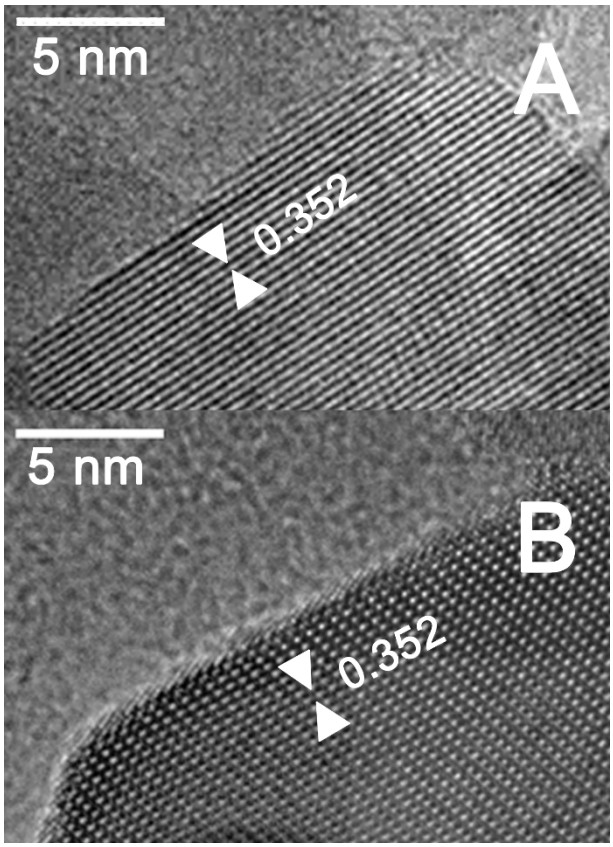

Figure 1. Fabbiani et al.

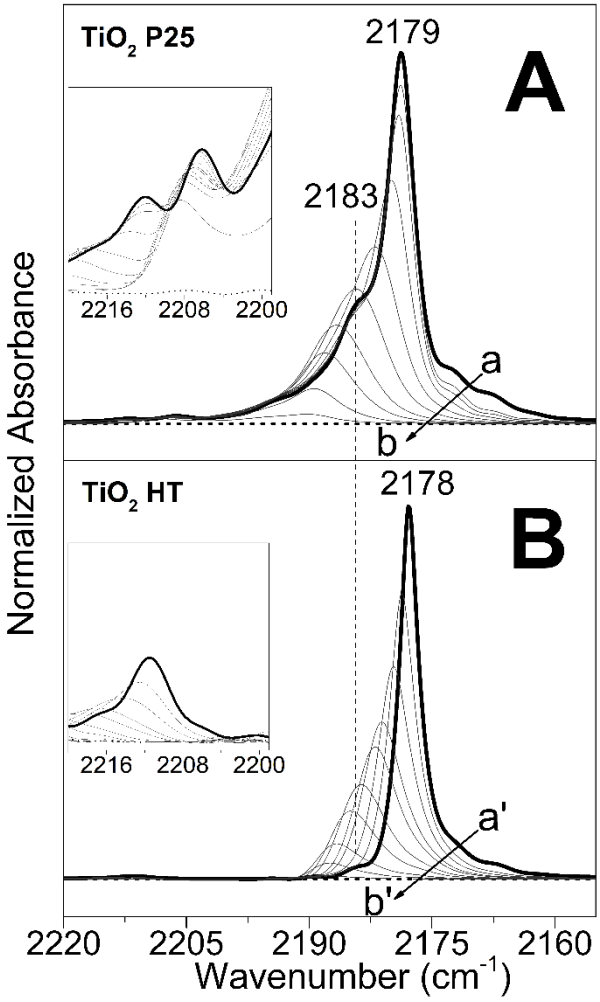

Figure 2. Fabbiani et al.

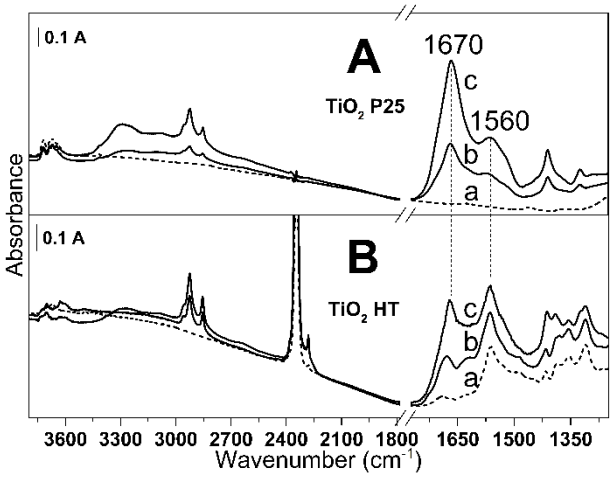

Figure 3. Fabbiani et al.

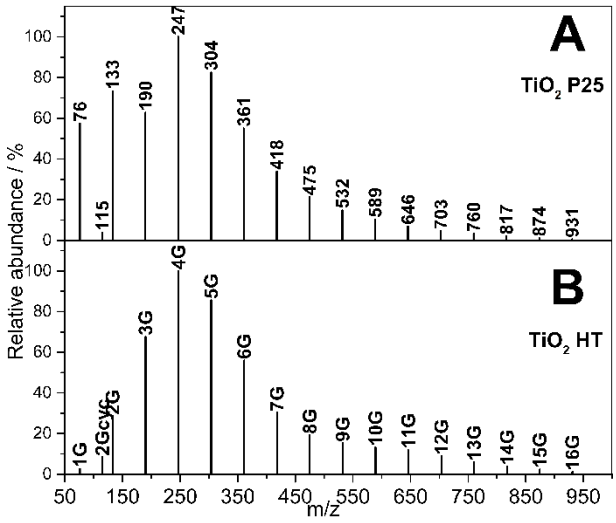

Figure 4. Fabbiani et al.

References

1. S. L. Miller and J. L. Bada, *Nature*, 334, 609 **(1988)**.
2. J. P. Ferris, A. R. Hill, R. Liu and L. E. Orgel, *Nature*, 381, 59 **(1996)**.
3. V. R. Pattabiraman and J. W. Bode, *Nature*, 480, 471 **(2011)**.
4. M. Rodriguez-Garcia, A. J. Surman, G. J. T. Cooper, I. Suárez-Marina, Z. Hosni, M. P. Lee and L. Cronin, *Nature*, 6, 8385 **(2015)**.
5. S. W. Fox and K. Harada, *J. Am. Chem. Soc.*, 82, 3745 **(1960)**.
6. J. D. Bernal, *Proc. Phys. Soc., London, Sect. B*, 62, 597 **(1949)**.
7. L. E. Orgel, *Origins Life Evol. Biospheres*, 28, 227 **(1998)**.
8. A. Rimola, D. Costa, M. Sodupe, J.-F. Lambert and P. Ugliengo, *Chem. Rev.*, 113, 4216 **(2013)**.
9. M. Meng, L. Stievano and J.-F. Lambert, *Langmuir*, 20, 914 **(2004)**.
10. J. Bujdák and B. M. Rode, *J. Mol. Evol.*, 45, 457 **(1997)**.
11. P. Leyton, R. Saladino, C. Crestini, M. Campos-Vallette, C. Paipa, A. Berríos, S. Fuentes and R. A. Zárate, *Amino Acids*, 42, 2079 **(2012)**.
12. S. Pantaleone, A. Rimola and M. Sodupe, *J. Phys. Chem. C*, 121, 14156 **(2017)**.
13. J.-F. Lambert, *Origins of Life and Evolution of Biospheres*, 38, 211 **(2008)**.
14. J. Bujdak and B. M. Rode, *J. Mol. Evol.*, 43, 326 **(1996)**.
15. G. Martra, C. Deiana, Y. Sakhno, I. Barberis, M. Fabbiani, M. Pazzi and M. Vincenti, *Angew. Chem. Int. Ed.*, 53, 4671 **(2014)**.
16. H.-J. Freund, *Faraday Discuss.*, 114, 1 **(1999)**.
17. U. Aschauer, Y. He, H. Cheng, S.-C. Li, U. Diebold and A. Selloni, *J. Phys. Chem. C*, 114, 1278 **(2010)**.
18. X.-Q. Gong, A. Selloni, M. Batzill and U. Diebold, *Nat. Mater.*, 5, 665 **(2006)**.
19. C. Deiana, E. Fois, G. Martra, S. Narbey, F. Pellegrino and G. Tabacchi, *ChemPhysChem*, 17, 1956 **(2016)**.
20. C. Deiana, M. Minella, G. Tabacchi, V. Maurino, E. Fois and G. Martra, *Phys. Chem. Chem. Phys.*, 15, 307 **(2013)**.
21. K. I. Hadjiivanov and G. N. Vayssilov, in *Advances in Catalysis*, edited B. C. Gates and H. Knozinger, Elsevier Academic Press Inc, San Diego (2002), Vol. 47, pp. 307.
22. G. Martra, *Appl. Catal., A*, 200, 275 **(2000)**.
23. C. Morterra, *J. Chem. Soc., Faraday Trans. 1*, 84, 1617 **(1988)**.
24. K. Hadjiivanov, J. Lamotte and J.-C. Lavalley, *Langmuir*, 13, 3374 **(1997)**.
25. C. Deiana, G. Tabacchi, V. Maurino, S. Coluccia, G. Martra and E. Fois, *Phys. Chem. Chem. Phys.*, 15, 13391 **(2013)**.
26. C. Arrouvel, M. Digne, M. Breysse, H. Toulhoat and P. Raybaud, *J. Catal.*, 222, 152 **(2004)**.
27. C. Deiana, E. Fois, S. Coluccia and G. Martra, *J. Phys. Chem. C*, 114, 21531 **(2010)**.